



# Crack Detection in Concrete Parts Using Vibrothermography

Yu Jia<sup>1,2,4</sup> · Lei Tang<sup>1,4</sup> · Binhua Xu<sup>1,3,4</sup> · Shenghang Zhang<sup>1,4</sup>

Received: 11 September 2018 / Accepted: 2 February 2019 / Published online: 7 February 2019  
© Springer Science+Business Media, LLC, part of Springer Nature 2019

## Abstract

This study investigates the use of vibrothermography to detect cracks in concrete parts, developing acoustic excitation devices (sonic and ultrasonic and low- and high-power excitation devices) and examining the influences of excitation frequency, power, and pressure on the ability to detect cracks. Experimental results demonstrate that this inspection technique can suitably detect concrete cracks: Ultrasound at frequencies from 20 to 100 kHz could be used to excite concrete cracks with notable temperature rise; coarse aggregates in concrete do not interfere with the ability to detect cracks; high-power ultrasound enhances crack detection though intense scattering of attenuation that could be induced by coarse aggregates. Moreover, the stimulus horn designed as part of this study can input ultrasound at high power into concrete parts without damaging the contact surface, while the custom-made pressure loading sleeve can steadily exert force on the transducer during excitation; the optimal force exerted on KMD ultrasonic transducers with a rated power of 50 W is ~ 1500 N, which can make the transducer output enough power to detect cracks.

**Keywords** Acoustic excitation device · Concrete material · Crack detection · Vibrothermography

## 1 Introduction

The potential of a novel non-destructive technique called vibrothermography which is used to detect surface and near surface defects has aroused wide industrial interest [1]; this technique involves ultrasound stimulation that induces a temperature gradient between defects and non-defective areas in materials under inspection. The detection system consists of an ultrasonic generator, ultrasonic transducer, and infrared thermal imager. The ultrasonic generator converts an electricity supply into a high-frequency alternating current (AC) signal and inputs it to the ultrasonic transducer [2]. Transformed from the AC signal, mechanical fluctuations in the ultrasonic frequency are generated by the transducer.

Then, the ultrasound passes into the object to be inspected through an interface between the object and the transducer. When the ultrasound propagates through defects, heat is generated from the conversion of attenuated ultrasonic energy and accumulates along defects in the form of a temperature increase. The temperature field of the inspected object is observed with an infrared thermal imager, and regions showing a significant temperature rise are analysed with software to identify the presence of defects.

Vibrothermography is advantageous in that large areas around a single stimulation point can be inspected quickly; thus, this technique has been widely researched. For example, Cho et al. [3] applied vibrothermography to the detection of groove defects in copper and CFRP pipes; Mian et al. [4] to assessing fatigue damage in graphite/epoxy composites; Guo et al. [5] to inspecting cracks in heavy aluminium aircraft structures, effectively detecting closed cracks; Robin et al. [6] to detecting emerging cracks in massive steel components; and Piau et al. [7] to testing open microscopic cracks in plasma-sprayed coatings that were fabricated via a controlled bending test.

Concrete is widely used as a building material for structural components. Cracking is a common defect that occurs in concrete structures during their service life [8]; structural failure in key components such as girders or

---

✉ Lei Tang  
ltang@nhri.cn

<sup>1</sup> Nanjing Hydraulic Research Institute, Nanjing 210029, China

<sup>2</sup> College of Water Conservancy and Hydropower Engineering, Hohai University, Nanjing 210098, China

<sup>3</sup> College of Civil and Transportation Engineering, Hohai University, Nanjing 210098, China

<sup>4</sup> State Key Laboratory of Hydrology-Water Resources and Hydraulic Engineering, Nanjing 210029, China

load-bearing columns can easily be induced by crack expansion. Early detection of cracks—followed by appropriate repair—is essential to preventing crack expansion and ensuring structural safety [9]. Cracking is a discontinuous defect and is generally distributed in a disordered manner in concrete structures. Discontinuous areas with a high temperature rise can be distinguished by the naked eye in a thermal image after several seconds of inspection; thus, the shape and distribution of defects can be visually displayed; this ability makes the application of vibrothermography to detecting concrete cracks worth researching. In contrast to homogeneous and isotropic materials, such as metals, polymer-based materials, composite materials, and carbon-fibre-reinforced plastics, concrete—which is a composite of sand and coarse aggregates embedded into a cement paste matrix—cannot be assumed to be non-dispersive [10]. Concrete's brittleness may allow a test surface to be damaged by an excitation device before the excitation waves have been input into the object to be inspected. When excitation waves are transmitted into the object, interactions with aggregates may modify the propagating behaviour of the waves via multiple scattering, so that the relevant attenuation of the waves accompanies the scattering [11, 12]. The attenuated energy is eventually converted into heat; it is therefore likely that temperature increases at defects are masked by those generated by interactions with coarse aggregates.

Thus, in this study, the authors investigate the applicability of vibrothermography to concrete crack detection. Ultrasound excited systems are constituted, some with new component designs. Excitation experiments conducted focus on influence of the excitation frequency, power, and pressure on crack detection ability. The results are analysed to ascertain the feasibility of applying this method to crack detection in concrete.

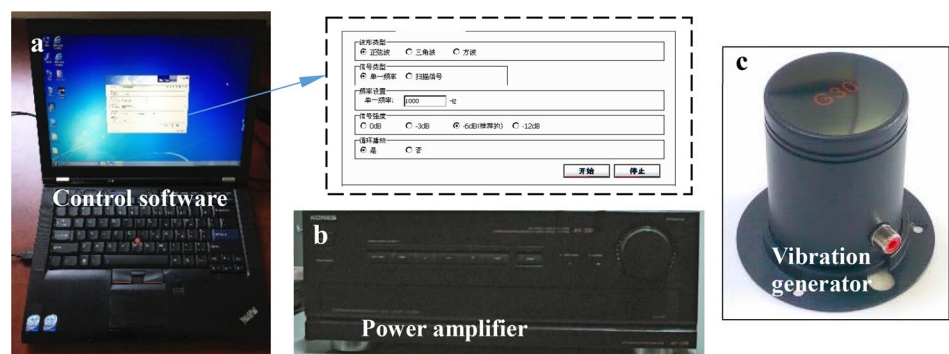
## 2 Acoustic Excitation System

Three sets of acoustic excitation devices were developed and used to inspect concrete cracks. Because coarse aggregates exist in the cement paste matrix, ultrasound—with a frequency higher than that of sound—can be easily attenuated while propagating in the concrete. Therefore, an acoustic generation system was established to output sound at frequencies between 150 and 12,000 Hz. In accordance with vibrothermography concepts applied to metals and composite materials, this study produced an ultrasonic excitation system with a rated power of 50 W and tuneable frequencies ranging from 20 to 100 kHz. In addition, should the ultrasound energy generated from the 50 W transducer, after attenuation by coarse aggregates in the concrete, be too low to detect cracks, excitation experiments were also conducted using a high-power 20 kHz ultrasonic excitation system that is tuneable from 100 to 1000 W.

### 2.1 Acoustic-Frequency Excitation System

A transducer driven at a power of approximately 50 W has been successfully applied to detecting tip cracks in an aero-engine blade [13]; in accordance with these earlier results, this study employed an acoustic generation system driving a 60 W exciter. Figure 1 shows the system, which consisted of control software installed in a computer that operated a G30 vibration generator (with a power rating of 60 W) tuneable to frequencies of 150–12000 Hz and a KONESAV-338 power amplifier with a rated power of 500 W that amplified the electric signal output from the computer to drive the G30 exciter. The G30 vibration generator (Gansu Tianxing High-Tech Company in Lanzhou, China) is pressed on an inspected object surface and outputs a continuous sinusoidal wave. When conducting experiments, the actuator output one-single-frequency wave at one experiment.

**Fig. 1** Acoustic-frequency excitation system: **a** a computer installed with acoustic-frequency control software, **b** power amplifier, **c** G30 vibration generator



## 2.2 Ultrasonic-Frequency Excitation System with Tuneable Frequency

The ultrasonic generation system involved an ultrasonic generator tuneable at frequencies between 28 and 100 kHz with matching 28, 40, 68, 80, and 100 kHz transducers with a rated power of 50 W. Combined with the acoustic-frequency excitation system, the ultrasonic system, featuring a range of ultrasonic frequencies and a low output power, was also used to explore the influence of excitation frequencies (greater than 20 kHz) on the detection of cracks. The ultrasonic system is shown in Fig. 2. The ultrasonic generation systems were manufactured by Shenzhen KMD Ultrasonic Equipment Co., Ltd.; the transducers used in the following experiments were KMD-2850, KMD-4050, KMD-6850, KMD-8050, and KMD-10050 corresponding to excitation frequencies of 28, 40, 68, 80, and 100 kHz, respectively.

Stable and durable excitation of the transducers is necessary for excitation experiments [14]. Thus, it is critical to appropriately attach the transducers to the object to be inspected for all power ultrasound applications [15]. A pressure loading sleeve was designed for the transducers shown in Fig. 2, serving as an auxiliary device that is glued on the object's surface to firmly attach it to the sleeve and enable subsequent load application. The sleeve consists of a main structure and fabricated spacing rings. The lift-able axle in the main structure, mounted with flanges, is designed to exert force and spacing rings are designed to match the various transducer diameters. With this sleeve, forces generated on the object surface can be balanced. From the force diagram in Fig. 2b, pressure  $F_1$ , generated by the

axle's effect on the transducer, equalled tension  $F_2$ , generated by the sleeve's effect on the bonding surface. Hence, forces exerted on a crack in the object did not increase after the sleeve provided force on the transducer.

A 4.9 kN button force sensor was embedded between the axle and transducer in the sleeve to measure the force exerted on the transducer during excitation.

## 2.3 Ultrasonic-Frequency Excitation System with High Excitation Power

The high-powered ultrasonic generation system was PLD-6040, manufactured by Suzhou PLD Precision Machinery Co., Ltd., which included an ultrasonic generator at a frequency 20 kHz with a matching 20 kHz transducer with a power range of 100–1000 W, as shown in Fig. 3. This system was used to avoid failures in crack detection due to insufficient vibration displacements in the object to be inspected.

A pressure-controlled system was integrated in the device; this system consisted of a magnetic valve, air cylinder, air supply, and throttle valve. Together, the first three components raise and lower the stimulus horn; the throttle valve controls the total force exerted on the horn, as well as its descent rate. The pressure-controlled system is driven by a circuit board embedded in the ultrasound generator.

The stimulus horn, shown in Fig. 3d, was newly designed. It is a key element of the ultrasonic excitation device [16]. The specific geometry and material of the horn influence the function and operation of the transducers and control the actual frequencies and amplitude of the output ultrasound [15]. The horn's material also determines whether ultrasonic

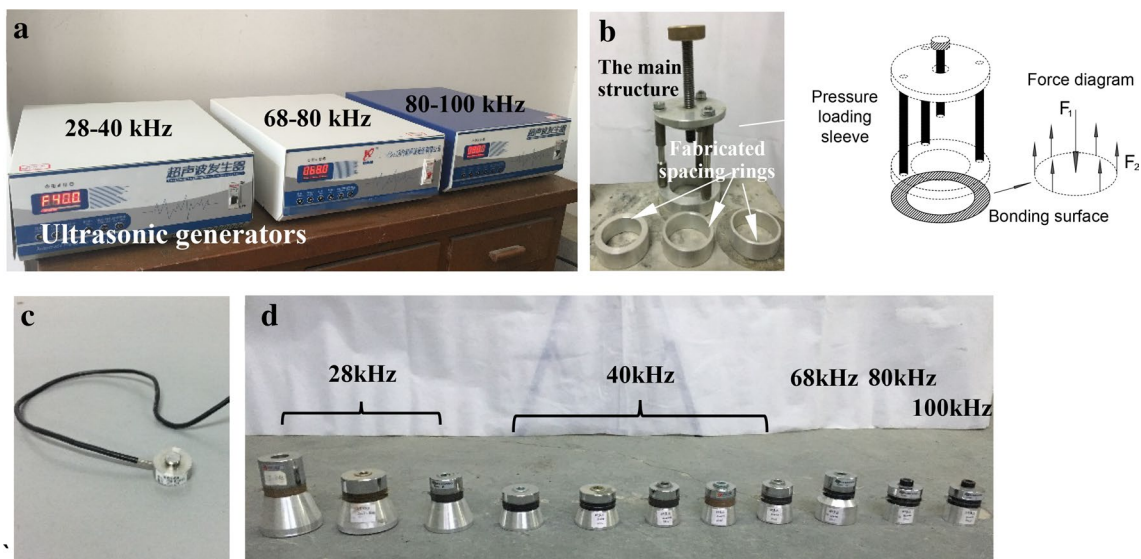


**Fig. 2** Ultrasonic excitation system with tuneable excitation frequencies: **a** 28–40, 68–80, and 80–100 kHz ultrasonic generators, **b** pressure loading sleeve and force diagram of its bonding surface, **c** 4.9

kN button force sensor, **d** 28–100 kHz ultrasonic transducers with a power rating of 50 W

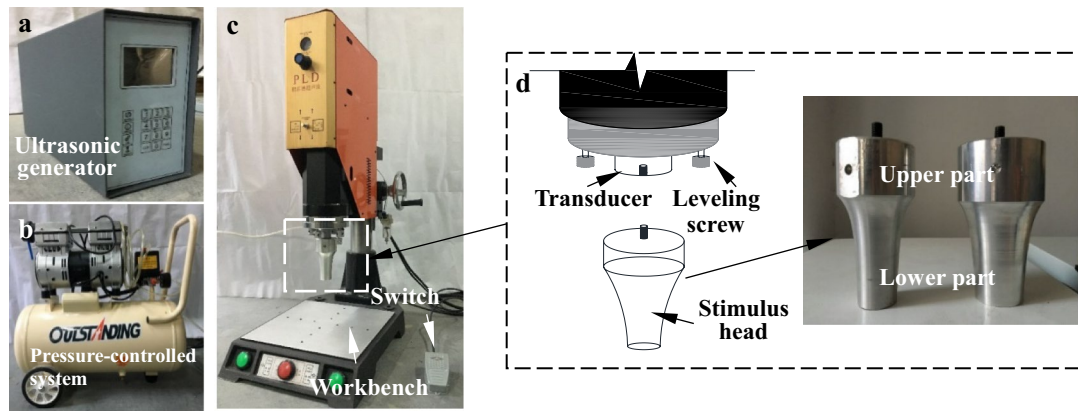


**Fig. 3** Ultrasonic excitation system with tuneable excitation power: **a** 20 kHz ultrasonic generator, **b** pressure-controlled system, **c** excitation table with controllable pressure, **d** decomposition of the transducer and stimulus horn

**Table 1** Concrete mix proportions

Strength design grade	Water–cement ratio	Slump (mm)	Sand rate (%)	Amount of material used per cubic meter concrete (kg)			
				Water	Cement	Sand	Stone
C30	0.52	55–70	33.5	205	398	605	1202

energy could be transmitted into concrete, as well as the degree of dissipation in ultrasonic energy when propagating through the horn. Given the acoustical impedance characteristics of concrete materials, an aluminium alloy was selected for the horn. The horn was designed to be symmetrical about the horizontal plane, to eliminate parasitic transversal vibration components along the vertical direction [15]. In addition, the stepped cylinder form of the horn permits the highest possible ultrasonic amplification [17]. The length of the horn is 130 mm and the ratio between the upper and lower parts is 0.53: the diameter of the upper section is 78 mm and the diameter of the working end of the lower part is 45 mm.

### 3 Acoustic Excitation Experiments

#### 3.1 Test Samples

Concrete and cement mortar were used to fabricate the experimental samples. Concrete samples consisted of ordinary Portland cement (P.O. 42.5) with 5–31.5 mm gravel and continuous gradation; the mix proportions are presented in Table 1. Cement mortar samples (P.O. 42.5) were prepared with water–cement and cement–sand ratios of 1:2 and 1:3, respectively; ISO standard sand complying with GB178-77 was used as fine aggregate [18]. The mixture proportions are shown in Table 2.

Two kinds of C30 concrete samples containing cracks fabricated using different loading method were

**Table 2** Cement mortar mix proportions in kg/m<sup>3</sup>

Cement	Fine aggregate	Water
586	1758	298

used in these experiments. Using three-point bending, a transverse crack was produced in the middle of a 250 mm × 100 mm × 100 mm sample that penetrated the upper surface of the sample, shown in Fig. 4a. A transverse crack was also produced in the middle of a 430 mm × 400 mm × 100 mm specimen, this time using the wedge-splitting method, and is shown in Fig. 4b. Although both samples contained transverse cracks, they were not broken apart entirely. A 250 mm × 100 mm × 100 mm cement mortar sample with no cracks was also used.

The dimensions of cracks on the monitoring surface of the samples are shown in Table 3. The directions of the crack widths, lengths, and depths in the samples are defined in the coordinate systems in Fig. 4. Because the width of the surface crack varied along its length, it was hard to identify the width of each point in the surface crack. Therefore, only the ranges of the surface crack’s width were measured, which was sufficient for qualitative analysis of crack detection ability at various excitation frequencies.

#### 3.2 Thermal Image Acquisition System

A TH9100MV infrared thermal imager, which included an uncooled focal plane array detector (NEC) featuring a

320×240 pixel focal plane array and a frame frequency of 60 frames/s, was used to capture the temperature fields of the sample. The imager had a precision of 0.06 °C within the range of 0–250 °C [19]. Data from the thermal images were acquired with InReC Analyzer NS9500 standard software. The temperature field acquisition system is shown in Fig. 5.

### 3.3 Experiment Context

Concrete crack detection using vibrothermography was investigated considering three factors: excitation frequency,

power, and pressure. Sound and ultrasound are mechanical waves that generate compression and shear movements in concrete [20]. To mark defects in thermal images, vibrothermography relies on conversion of the attenuated mechanical waves that accumulate in defects into heat. Frequency and amplitude are important physical parameters of the mechanical waves that characterize the fluctuation state of the waves that influence heat generation. The excitation frequency determines the frequency of the mechanical wave transmitted in the object to be inspected; the excitation power and pressure influence the amplitude of this wave. Therefore,

**Fig. 4** Test samples: **a** concrete sample cracked by pressure loading (sample 1), **b** concrete sample cracked by split-tension loading (sample 2), **c** intact cement mortar sample (sample 3)

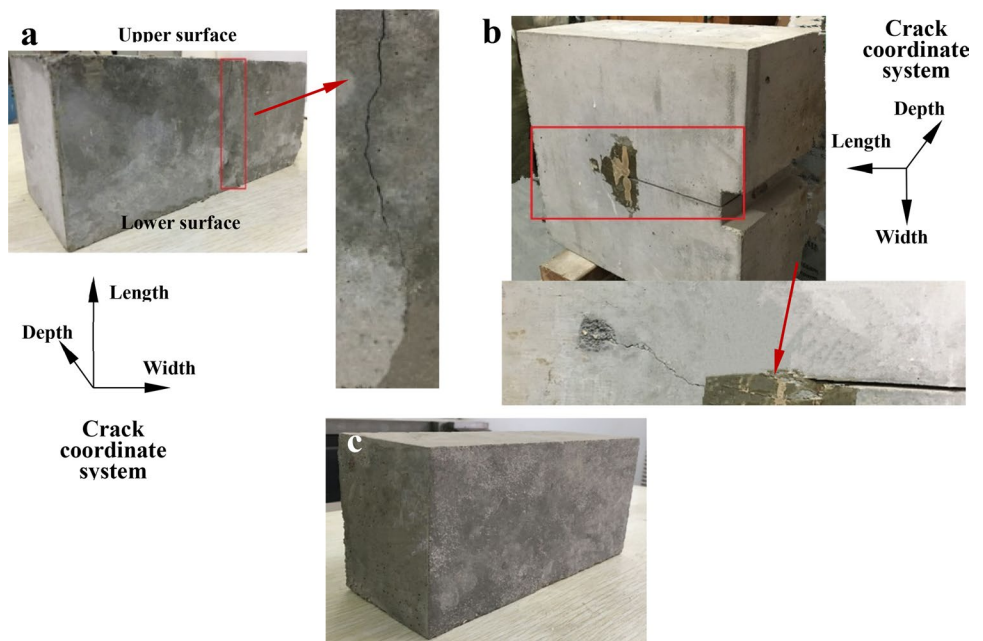
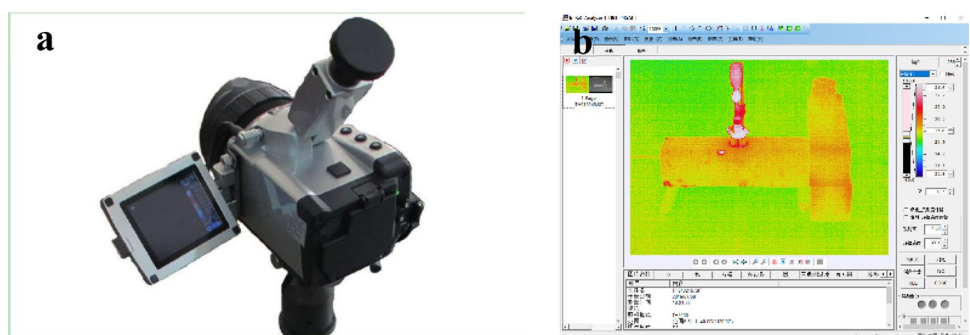


**Table 3** Parameters of cracks on monitoring surface

No.	Loading method	Orientation	Depth (mm)	Length (mm)	Width (mm)
1	Pressure loading	Penetrating through the sample along its depth and expanding from the upper surface to the lower surface	100	~100	0.06–0.23
2	Split-tension loading	Penetrating through the sample along its depth, originating from the precast crack and expanding obliquely upward along the sample length	100	~350	0.03–0.38

**Fig. 5** Temperature field acquisition system: **a** TH9100MV infrared thermal imager, **b** InReC Analyzer NS9500PRO standard software



the feasibility of vibrothermography for detecting concrete cracks can be verified by conducting excitation experiments surrounding the key parameters. In addition, numerous interfaces exist between the coarse aggregates and cement paste matrix, potentially causing the interface to interfere with the detection of cracks, as the interfaces can convert ultrasound energy into heat. Therefore, a cement mortar sample was excited for comparison with the concrete samples.

First, excitation waves at frequencies ranging from sonic to ultrasonic were generated for use on samples 1 and 3. The acoustic generation device was used to output continuous waves at frequencies between 150 and 12,000 Hz, and the ultrasonic generation device was used to generate ultrasounds of 28, 40, 68, 80, and 100 kHz. When the acoustic generation device was used, the excitation frequencies increased at intervals of 1000 Hz from 150 to 12,000 Hz, so that twelve sets of acoustic-excitation experiments were conducted.

Second, excitation waves with low and high power were generated for use on sample 2. Ultrasounds of 20 kHz were generated by the ultrasonic transducer at powers of 200, 300, and 600 W. The experiments were used to examine whether the horn could input high-power ultrasound into the samples without damaging the test surface and to determine the influence of high excitation power on crack detection.

Third, vibrothermography results often suffer from bad repeatability due to the force exerted on the transducer [14], so the influence of the excitation force on crack detection was studied using sample 2. The tuneable-frequency

ultrasonic generation device that matched transducers with a rated power of 50 W was used. Transducers were operated with an applied force from 500 to 2500 N, in increments of 500 N. A pressure loading sleeve was glued on the sample surface for secure attachment and to apply force.

Only a single-frequency ultrasound was used in each excitation experiment because corresponding ultrasonic devices were convenient and commercially available [21]. In addition, as tight contact is beneficial for efficiently imparting ultrasound energy into samples (reducing harmonic generation from hammering effects of the transducer into the sample surface) [22], the transducers were placed on a smooth clean sample surface and force was exerted on the transducers during the excitation experiments.

## 4 Results and Discussion

### 4.1 Excitation Frequency

As mentioned previously, twelve groups of acoustic-excitation and five groups of ultrasonic-excitation experiments were conducted on sample 1 and five groups of ultrasonic-excitation experiments on the cement mortar sample 3 were conducted. The experimental conditions are shown in Table 4. The cement mortar sample was used to conduct contrast tests, so the conditions of only one excitation experiment (68 kHz excitation experiment chosen from experiments with excitation frequencies of 28, 40, 68, 80,

**Table 4** Excitation experiment conditions

No.	Sample tested	Excitation frequency (kHz)	Excitation time (s)	Contact force (kN)	RMS current (A)	Output power (W)
1	1	0.15	15	2	~0.6	~80
		1.15				
		2.15				
		3.15				
		4.15				
		5.15				
		6.15				
		7.15				
		8.15				
		9.15				
		10.15				
		11.15				
2	1	28	15	2	0.21	~75
3	1	40	15	2	0.23	~80
4	1	68	15	2	0.18	~50
5	1	80	15	2	0.24	~60
6	1	100	15	2	0.23	~55
7	3	68	15	2	0.18	~50

and 100 kHz) are shown in Table 4. Different excitation positions were tried; when the excitation transducers were placed across the crack in its width direction on the sample's upper surface, notable temperature rises appeared in crack regions on the monitoring surface.

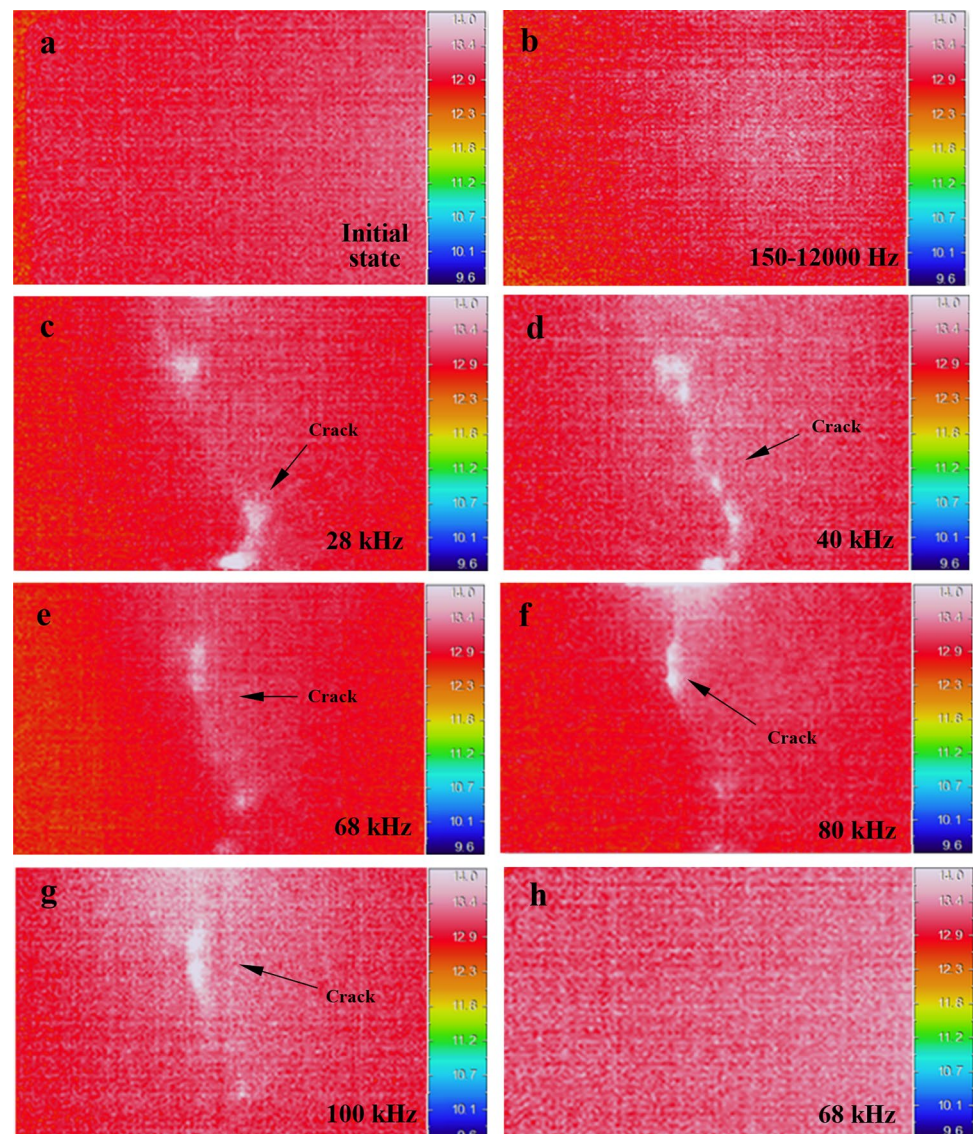
Results of excitation experiments are shown in the thermal images in Fig. 6. The thermal images were captured when the excitation lasted 15 s. Figure 6a shows a thermal image of sample 1 captured before excitation as a reference for those captured during excitation. Twelve groups of acoustic-excitation experiments (experiment 1 in Table 4) showed no significant differences; representative thermal images are shown in Fig. 6b. The cement mortar sample excited by 68 kHz ultrasound chosen as representative is shown in Fig. 6h.

In Fig. 6b, no notable areas of temperature increase could be discerned by the naked eye, whereas in Fig. 6c–g, areas

that contained cracks were excited with significant temperature rise. For example, the temperature of the crack was  $\sim 1.96^\circ\text{C}$  higher than that of the surrounding intact areas in Fig. 6c,  $\sim 2.01^\circ\text{C}$  higher in Fig. 6d,  $\sim 1.28^\circ\text{C}$  higher in Fig. 6e,  $\sim 1.78^\circ\text{C}$  higher in Fig. 6f, and  $\sim 1.75^\circ\text{C}$  higher in Fig. 6g. These temperature rises could be discerned by the naked eye. As per the experiment conditions in Table 4, excitation all lasted for 15 s and the output power of the acoustic generation device was no less than that of the ultrasound generation device. Thus, it can be inferred that mechanical waves of the ultrasonic frequencies could detect concrete cracks; further, they are more suitable to detecting concrete cracks with mouth-opening widths ranging from 0.06 to 0.23 mm than those of acoustic frequencies.

Comparing Fig. 6c–g with Fig. 6h, the intact areas in concrete sample 1 and cement mortar sample 3 both demonstrated a relatively uniform temperature and the colour

**Fig. 6** Thermal images of acoustic and ultrasonic excitation [a–g excitation of the concrete sample, h excitation of the cement mortar sample]: a initial state before excitation, b 150–12000 Hz sound, c 28 kHz ultrasound, d 40 kHz ultrasound, e 68 kHz ultrasound, f 80 kHz ultrasound, g 100 kHz ultrasound, h 68 kHz ultrasound



reflected by the temperature value in the thermal image could be regarded as the background colour of the cracked areas, even though the intact areas of sample 1 were full of coarse aggregates. It can be inferred that the coarse aggregates embedded in the cement paste matrix did not interfere with the crack detection ability of vibrothermography.

## 4.2 Excitation Power

Figure 7 shows the thermal images of concrete sample 2 excited by 20 kHz ultrasound with different powers. Figure 7b shows that the sample was excited by ultrasound with a power of 200 W for 3 s, Fig. 7c excited with 300 W for 2 s and Fig. 7d excited with 600 W power for 1 s. The pre-cast crack was excited with a temperature increase that could be discerned by the naked eye in the three thermal images; furthermore, the crack appeared increasingly distinctly from Fig. 7b–d (the crack temperature was 0.3–0.6 °C higher than the surrounding area in Fig. 7b, 0.5–0.8 °C higher in Fig. 7c, and 0.8–2.4 °C higher in Fig. 7d). It can be inferred that vibration displacements led by the 600 W excitation power in Fig. 7d were sufficiently larger, making the crack lighter than those in Fig. 7b, c. The results clearly show that high-power excitation is beneficial for detecting cracks in concrete, despite the excitation leading to intense attenuation of the ultrasound by coarse aggregate scattering.

As almost the whole crack was marked with clearly detectable temperature increases and the contact surface on

sample 2 was intact, it can be noted that the stimulus horn of the ultrasonic generating device succeeded in inputting high-power ultrasound into the sample without damaging the contact surface between the horn and the sample.

## 4.3 Excitation Pressure

The 40 kHz transducer with a rated power of 50 W was used to conduct excitation experiments for a representative case. Five groups of experiments were conducted with increasing force at intervals of 500 N from 500 to 2500 N. Thermal images were captured when the sample was excited for 30 s and are shown in Fig. 8. As duration of the excitation was 30 s, heat generated by the working transducers diffused into the samples and accumulated, which resulted in remarkable temperature rise concentrating at the excitation position.

The temperature increase of the crack in Fig. 8 differed across cases. When the sample was excited at forces of 500 N and 2500 N, the crack showed almost no temperature rise. At forces of 1000 N or 2000 N, the crack produced a temperature rise that could be discerned by the naked eye in the thermal image (the crack temperature was 0.2–0.6 °C higher than the surrounding area in Fig. 7c and 0.2–0.7 °C higher in Fig. 7e). For the sample excited at a force of 1500 N, the temperature rise of the crack was high and could be easily discerned (the crack temperature was 0.4–0.9 °C higher than the surrounding area). The results show that the

**Fig. 7** Thermal images of ultrasonic excitation with different powers: **a** initial state before excitation **b** 200 W power excitation for 3 s, **c** 300 W power excitation for 2 s, **d** 600 W power excitation for 1 s

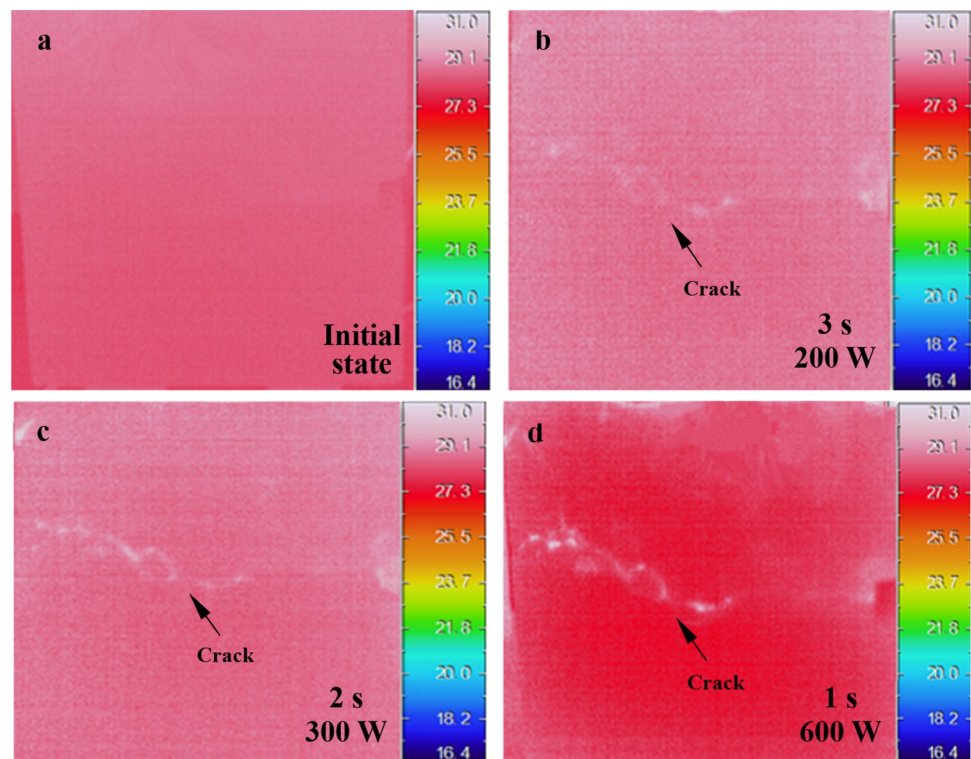
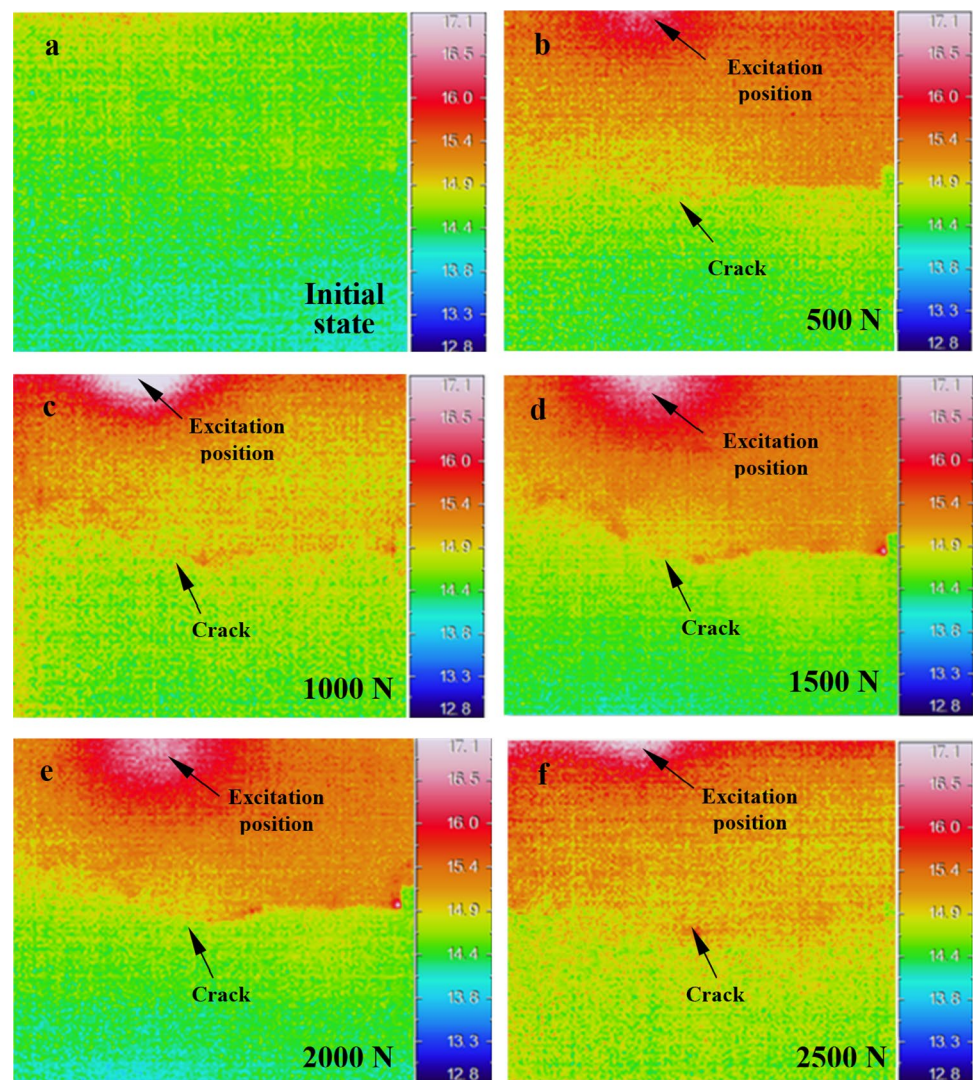




**Fig. 8** Thermal images of ultrasonic excitation under several forces: **a** initial state before excitation, **b** 500 N, **c** 1000 N, **d** 1500 N, **e** 2000 N, **f** 2500 N



concrete crack detection ability of vibrothermography is also influenced by excitation pressure.

According to the loading properties of the sleeve, the applied force was balanced on the inspected object's surface, so that force on the crack in sample 2 did not increase. Impedance matching was implemented to link the electrical driving system (the ultrasonic generator) and the transducer to improve transmission efficiency [23, 24], which can clarify why the temperature increase in cracks varied with excitation pressure. The transducer impedance can vary during excitation [25]; dynamic resistance of the 50 W KMD transducer increased with the increasing pressure exerted on the transducer [26]. When the transducer impedance reached a proper value relative to the internal resistance of the ultrasonic generator, the output power of the transducer was maximized. It is likely that when the 1500 N force was exerted on the transducer, satisfactory electrical matching of the transducer and ultrasonic generator was ensured, so that the transducer was at its optimum operation position.

Transducers of other frequencies (28, 68, 80, and 100 kHz), with a rated power of 50 W, displayed almost the same tendency shown in Fig. 8 when forces between 500 and 2500 N were applied. In addition, readings from the button force sensor were constant in each experiment. Therefore, crack detection ability improved when a force of ~1500 N was applied on KMD ultrasonic transducers with a power rating of 50 W; the custom pressure loading sleeve steadily exerted force on the transducers during excitation.

## 5 Conclusions

This study investigated the application of vibrothermography to the detection of cracks in concrete. Acoustic excitation systems, including acoustic-frequency and ultrasonic-frequency generating systems, were designed with which to conduct excitation experiments. Pre-cracked concrete samples were inspected in excitation experiments that were

conducted at varying excitation frequencies, powers, and pressures. The obtained results demonstrate the following:

- Vibrothermography can be applied to detecting cracks in concrete parts. Experimental evidence is presented to verify that ultrasound at frequencies from 20 to 100 kHz could be used to excite concrete cracks, producing a notable temperature rise. Scattering attenuation by coarse aggregates embedded into the cement paste matrix led to uniform distribution of the heat converted from the attenuated ultrasound energy in the concrete; the temperature rise in the cracks was not masked and could be discerned in thermal images.
- The newly designed stimulus horn succeeded in inputting the ultrasound at high power levels into concrete parts without damaging the contact surface between the horn and concrete. In addition, the high-power ultrasound indeed enhanced the ability to detect cracks, even though intense scattering attenuation could be also induced by coarse aggregates.
- The custom-made pressure loading sleeve could steadily exert force on the 50 W KMD transducer at frequencies of 28, 40, 68, 80, and 100 kHz during excitation. The optimal force for detection by the 50 W KMD transducers was approximately 1500 N.

This work verified the ability of vibrothermography to detect cracks in concrete, looking toward the ultimate goal of controlling such cracks. Further avenues for research may include exploring the heat-generating mechanisms of the vibrating concrete cracks; enlarging the detection ranges of current technology; and clarifying the relationship between temperature increases and crack opening widths, which can be conducted, for example, by exerting tensile or compressive forces on cracks to examine how asperity-contact-generated heating can be turned on or off [27], and by using a mix of frequencies or a frequency-modulated sinusoidal wave (instead of mono-frequent excitation) to investigate whether low-power stimulation may produce detectable temperature signals at cracks in concrete [22].

**Funding** This work was supported by the National Natural Science Foundation of China (Grant No. 51527811) and the National Key Research and Development Plan of China (Grant No. 2016YFC0401610).

## References

1. Renshaw, J., Chen, J.C., Holland, S.D., Thompson, R.B.: The sources of heat generation in vibrothermography. *NDT and E Int.* **44**(8), 736–739 (2011). <https://doi.org/10.1016/j.ndteint.2011.07.012>
2. Khmelev, V.N., Barsukov, R.V., Slivin, A.N., Tchyganok, S.N.: System of phase-locked-loop frequency control of ultrasonic generators. In: Proceedings 2nd Annual Siberian Russian Student Workshop on Electron Devices and Materials (2001) <https://doi.org/10.1109/SREDM.2001.939147>
3. Cho, J.W., Seo, Y.-C., Jung, S.-H., Jung, H.-K.: Defect detection within a pipe using ultrasound excited thermography. *Nucl. Eng. Technol.* **39**(5), 637–646 (2007). <https://doi.org/10.5516/NET.2007.39.5.637>
4. Mian, A., Han, X., Islam, S., Newaz, G.: Fatigue damage detection in graphite/epoxy composites using sonic infrared imaging technique. *Compos. Sci. Technol.* **64**(5), 657–666 (2004). <https://doi.org/10.1016/j.compscitech.2003.07.005>
5. Guo, X., Vavilov, V.: Crack detection in aluminum parts by using ultrasound-excited infrared thermography. *Infrared Phys. Technol.* **61**, 149–156 (2013). <https://doi.org/10.1016/j.infrared.2013.08.003>
6. Plum, R., Ummenhofer, T.: Use of ultrasound excited thermography applied to massive steel components emerging crack detecting methodology. *J. Bridge Eng.* **18**(6), 455–463 (2013). [https://doi.org/10.1061/\(ASCE\)BE.1943-5592.0000355](https://doi.org/10.1061/(ASCE)BE.1943-5592.0000355)
7. Piau, J.-M., Bendada, A., Maldague, X., Legoux, J.-G.: Non-destructive testing of open microscopic cracks in plasma-sprayed-coatings using ultrasound excited vibrothermography. *Nondestruct. Test. Eval.* **23**(2), 109–120 (2008). <https://doi.org/10.1080/10589750701775817>
8. De Belie, N., De Muynck, W.: Crack repair in concrete using biodeposition. In: Proceedings of the 2nd International Conference on Concrete Repair, Rehabilitation and Retrofitting, pp. 291–292 (2008)
9. Wan, K.T., Leung, C.K.Y.: Fiber optic sensor for the monitoring of mixed mode cracks in structures. *Sens. Actuators A* **135**(2), 370–380 (2007). <https://doi.org/10.1016/j.sna.2006.08.002>
10. Philippidis, T.P., Aggelis, D.G.: Experimental study of wave dispersion and attenuation in concrete. *Ultrasonics* **43**(7), 584–595 (2005). <https://doi.org/10.1016/j.ultras.2004.12.001>
11. Chaix, J.F., Garnier, V., Corneloup, G.: Ultrasonic wave propagation in heterogeneous solid media: theoretical analysis and experimental validation. *Ultrasonics* **44**(2), 200–210 (2006). <https://doi.org/10.1016/j.ultras.2005.11.002>
12. Waterman, P.C., Truell, R.: Multiple scattering of waves. *J. Math. Phys.* **2**(4), 512–537 (1961). <https://doi.org/10.1063/1.1703737>
13. Homma, C., Rothenfusser, M., Baumann, J., Shannon, R.: Study of the heat generation mechanism in acoustic thermography. *Proc. AIP Conf.* **820**, 566 (2006). <https://doi.org/10.1063/1.2184578>
14. Umar, M.Z., Vavilov, V., Abdullah, H., Ariffin, A.K.: Ultrasonic infrared thermography in non-destructive testing: a review. *Rus. J. Nondestruct. Test.* **52**(4), 212–219 (2016)
15. Parrini, L.: Design of advanced ultrasonic transducers for welding devices. *IEEE Trans. Ultrason. Ferroelectr. Freq. Control* **48**(6), 1632–1639 (2001). <https://doi.org/10.1109/58.971714>
16. Volkov, S.S., Kholopov, Y.V.: Technology and equipment for ultrasound welding structures made of polymer-based composite materials. *Weld. Int.* **12**(5), 400–403 (1998)
17. Millner, R.: *Ultraschalltechnik*. Physik-Verlag, Belin, Weinheim (1987)
18. GB178-1977 (2006) Standard Sand for Cement Strength Test. China Standard Press, Beijing
19. Lei, T., Hong, L., Yu, J., Ling, G.: Study of an acoustic field simulation of a temperature field excited by ultrasonic waves through a concrete specimen. *Insight* **59**(6), 305–310 (2017)
20. Garnier, V., Piwakowski, B., Abraham, O., Villain, G., Payan, C., Chaix, J.F.: Acoustic techniques for concrete evaluation: improvements, comparisons and consistency. *Constr. Build.*

- Mater. **43**, 598–613 (2013). <https://doi.org/10.1016/j.conbuildmat.2013.01.035>
21. Hiremath, S.R., Mahaoatra, D.R., Srinivasan, S.: Detection of crack in metal plate by thermo sonic wave based detection using FEM. *Exp. Stroke Transl. Med.* **1**(1), 12–18 (2012)
  22. Zweschper, T., Dillenz, A., Riegert, G., Scherling, D., Busse, G.: Ultrasound excited thermography using frequency modulated elastic waves. *Insight* **45**(3), 178–182 (2003)
  23. Chen, Y.-C., Wu, S., Chen, P.-C.: The impedance-matching design and simulation on high power electro-acoustical transducer. *Sens. Actuators, A* **115**(1), 38–45 (2004). <https://doi.org/10.1016/j.sna.2004.01.063>
  24. Inoue, T., Sasaki, T., Miyama, T., Sugiuchi, K.: Equivalent circuit analysis for Tonpiliz piezoelectric transducer. *IEICE Trans.* **E70**(10), 909–917 (1987)
  25. Martin, G.E.: On the theory of segmented electromechanical systems. *J. Acoust. Soc. Am.* **36**(7), 1366–1370 (1964). <https://doi.org/10.1121/1.1919209>
  26. Chen, Z.: Research of Ultrasonic Generator. Dissertation, Zhejiang University (2007)
  27. Lu, J., Han, X., Newaz, G., Favro, L.D., Thomas, R.L.: Study of the effect of crack closure in sonic infrared imaging. *Nondestruct. Test. Eval.* **22**(2–3), 127–135 (2007)

**Publisher's Note** Springer Nature remains neutral with regard to jurisdictional claims in published maps and institutional affiliations.